Detailed study of the Fourier transform of the time-interval photon statistics distribution applied to laser Doppler velocimetry

M. A. Rebolledo, J. M. Alvarez, and J. C. Amaré
Departamento de Física Aplicada, Facultad de Ciencias, Universidad de Zaragoza, 50009 Zaragoza, Spain
(Received 16 March 1988)

In this paper a technique consisting of measuring the Fourier transform Q_F of the time-interval photon statistics distribution is studied when applied to laser Doppler velocimetry. It is supposed that a device that changes the Gaussian intensity profile of the laser beam into a uniform intensity profile is used. A theoretical model for a fluid with a constant velocity is obtained and verified by two ways: experimentally and by a computer-simulation method. Then the experimental conditions for which the signal can be approached to a Lorentzian curve and the error involved in the determination of the fluid velocity are studied from the theoretical model. It is concluded that the measurement of Q_F is a useful technique for very low intensities.

INTRODUCTION

In laser Doppler velocimetry (LDV) experiments where a low scattered intensity is obtained, correlators are frequently used to process the signal.[1] As the intensity of the analyzed light beam decreases, shot noise increases and a larger error is involved in obtaining information about the light beam from the intensity autocorrelation function $g^{(2)}(\tau)$. However, for very small intensities the time interval θ between two consecutive photopulses can be measured with good accuracy. Since for a light beam whose intensity oscillates with a period P the time-interval probability $W(\theta)$ oscillates with the same period, the measurement of the Fourier transform of $W(\theta)$ seems to be a more appropriate technique than the intensity correlation one to measure P.

The advantage of this technique was proved[2] for light beams with a square-wave intensity. Later[3] it was experimentally verified that this technique can be applied to process the signal in a LDV experiment. The aim of this paper is to make a more complete study of this technique when applied to LDV experiments. Since the technique is simplified if a device[4] that changes the Gaussian intensity profile of the laser beam into a uniform intensity profile is used, in this paper we shall suppose uniform intensity light beams are used.

THEORY

Let us consider a fluid with a constant velocity that is measured by means of a differential Doppler system, where two laser beams with uniform intensity produce an interference fringe system. When a seeded particle enters into the fringe system at the instant t_j the scattered intensity oscillates as a function of time as

$$I(t)=I_P\{1+V\cos[\omega_0(t-t_j)+\delta]\} \quad (t_j\le t\le t_j+\tau) , \tag{1}$$

where I_P is the mean intensity in an oscillation, V the visibility of the fringes, ω_0 the angular frequency of the oscillations, δ a phase factor that indicates the phase difference between the two laser beams at the beginning of the fringes, and τ the time that it takes the particle to cross the fringes.

We shall use a simple model where τ is a constant for all the particles. We shall suppose that only one seeded particle can be found in the fringe system. Since the detection of light by a photomultiplier is a Poisson process,[5] the time-interval probability $W(\theta)$ does not depend on δ. Bearing the preceding assumptions in mind, it is obvious that $W(\theta)$ must coincide for $\theta\le\tau$ with the time-interval probability that corresponds to a sinusoidal function

$$I(t)=I_P[1+V\cos(\omega_0 t+\delta)] \quad (-\infty<t<+\infty) . \tag{2}$$

For very low intensities τ can be assumed to be much smaller than $t_{j+1}-t_j$. Therefore time intervals corresponding to photons scattered by two different seeded particles can easily be eliminated and consequently $W(\theta)=0$ for $\theta>\tau$.

For a sinusoidal signal such as the one in Eq. (2) it is found[6] that

$$W(\theta)=I_P\exp(-I_P\theta)Y(\theta) , \tag{3}$$

where

$$Y(\theta)=[1+V^2\cos^2(\omega_0\theta/2)]I_0(Z) -[2V\cos(\omega_0\theta/2)+V^2/Z]I_1(Z) , \tag{4}$$

I_0 and I_1 being modified Bessel functions[7] and

$$Z=Z_M\sin(\omega_0\theta/2) , \tag{5}$$

where

$$Z_M=2I_PV/\omega_0 . \tag{6}$$

For a low scattered intensity the values of Z are small and we can use an approximate expression for $Y(\theta)$ as indicated in the Appendix. Since $W(\theta)=0$ for $\theta>\tau$, the Fourier transform of $W(\theta)$ can be calculated from

$$Q_F(\omega)=\int_0^\tau W(\theta)\cos(\omega\theta)d\theta \tag{7}$$

if Eqs. (3), (A7), and (A8) are taken into account. The resulting expression for $Q_F(\omega)$ is

$$Q_F(\omega)=\left[1+(1+V^2/2)\sum_{K=1}^{\infty}A_K-(V^2/2)\sum_{K=1}^{\infty}B_K\right]F_0(\omega)+(V^2/4)\left[1+\sum_{K=1}^{\infty}A_K\right][F_{-1}(\omega)+F_1(\omega)]$$
$$-(Z_MV/4)\left[1+\sum_{K=1}^{\infty}B_K\right][G_{-1}(\omega)-G_1(\omega)]+\tfrac{1}{2}(1+V^2/2)\sum_{K=1}^{\infty}C_K\sum_{l=1}^{K}(-1)^l\begin{bmatrix}2K\\K-l\end{bmatrix}[F_{-l}(\omega)+F_l(\omega)]$$
$$-(V^2/4)\sum_{K=1}^{\infty}D_K\sum_{l=1}^{K}(-1)^l\begin{bmatrix}2K\\K-l\end{bmatrix}[F_{-l}(\omega)+F_l(\omega)]$$
$$+(V^2/8)\sum_{K=1}^{\infty}C_K\sum_{l=1}^{K}(-1)^l\begin{bmatrix}2K\\K-l\end{bmatrix}[F_{-(l+1)}(\omega)+F_{(l+1)}(\omega)-F_{-(l-1)}(\omega)-F_{(l-1)}(\omega)]$$
$$-(Z_MV/8)\sum_{K=1}^{\infty}D_K\sum_{l=1}^{K}(-1)^l\begin{bmatrix}2K\\K-l\end{bmatrix}[G_{-(l+1)}(\omega)-G_{(l+1)}(\omega)-G_{-(l-1)}(\omega)+G_{(l-1)}(\omega)]\ , \tag{8}$$

where A_K, B_K, C_K, and D_K are defined in the Appendix and

$$F_n(\omega)=\{1-\exp(-I_P\tau)\cos[(\omega-n\omega_0)\tau]\}L^{(n)}(\omega)+\exp(-I_P\tau)\sin[(\omega-n\omega_0)\tau]D^{(n)}(\omega)\ , \tag{9}$$

$$G_n(\omega)=\exp(-I_P\tau)\sin[(\omega-n\omega_0)\tau]L^{(n)}(\omega)+\{1-\exp(-I_P\tau)\cos[(\omega-n\omega_0)\tau]\}D^{(n)}(\omega)\ , \tag{10}$$

$L^{(n)}$ and $G^{(n)}$ being Lorentzian and dispersion curves defined as

$$L^{(n)}(\omega)=I_P^2/[I_P^2+(\omega-n\omega_0)^2]\ , \tag{11}$$

$$D^{(n)}(\omega)=I_P(\omega-n\omega_0)/[I_P^2+(\omega-n\omega_0)^2]\ . \tag{12}$$

For very low intensities Z_M is small and the terms in Eq. (8) that contain G_n functions are negligible. If this condition is accomplished and the number of interference fringes in the LDV system is large, $\exp(-I_P\tau)$ is small and then the dispersion term in F_n is negligible. As an example, let us consider a signal where $I_P/\nu_0=0.1$ and $\tau=50/\nu_0$ (there are 50 interference fringes); in this case $Z_M=2.86\times10^{-2}$ and $\exp(-I_P\tau)=6.74\times10^{-3}$. Therefore for low intensities and a large number of interference fringes $Q_F(\omega)$ becomes a linear expansion of Lorentzian functions centered at $\omega=\pm n\omega_0$ ($n=0,1,2,\ldots$).

EXPERIMENTAL SETUP

In order to show the validity of the theoretical model studied in the preceding section we used the experimental setup schematized in Fig. 1. To obtain a light beam with an intensity such as the one in Eq. (1) we designed an electronic simulator (SIM) that supplied a current that was observed in the oscilloscope (OSC) and fed it into the light emitting diode (L). The intensity of the emitted light beam was attenuated by the filter (F) and two linear polarizers P_1 and P_2 and detected by a photon correlation system consisting of the photomultiplier (PM), amplifier-discriminator (AD), time-interval meter (TI, controlled by the computer, COM), and a frequency meter (FM) to measure the signal photocount rate.

The values of $P=1/\nu_0$, δ, and τ for the signal generated by the simulator [Eq. (1)] can be varied in the following way: $10.0\ \mu s\le P\le 99.9\ \mu s$, $-\pi\le\delta\le0$, $\tau=(l+x)P$, where $l=9+10K$ ($K=0,1,\ldots,9$), and $-0.5\le x\le0.5$. The arrival times t_j are random. The difference $t_{j+1}-t_j$ has an exponential distribution[1] and the mean value $\langle t_{j+1}-t_j\rangle$ can be varied. In order to measure I_P [Eq. (1)] the simulator was provided with a switch that changes the simulated LDV signal into a sinusoidal signal [Eq. (2)] with the same values of I_P, V, and ω_0. The mean value of the intensity of this signal gives us I_P. The time-interval meter can measure 10^4 consecutive samples of the time interval θ that are transferred to COM and processed to obtain $Q_F(\omega)$.

EXPERIMENTAL AND COMPUTER-SIMULATION CHECK OF THE THEORETICAL MODEL

To verify the validity of the theoretical model we made experimental measurements of the time interval θ for different experimental situations. In four cases we used these values of θ to calculate the histogram

$$H(l,\Delta)=\int_{(l-1)\Delta}^{l\Delta}W(\theta)d\theta\quad(l=1,2,\ldots,N_c) \tag{13}$$

and in six cases we used the values of θ to calculate $Q_F(\nu_l)$, with $\nu_l=\nu_i+(l-1)\Delta\nu$ ($l=1,2,\ldots,N_c$). In order to make a more complete verification of the theoretical model validity we used a computer-simulation

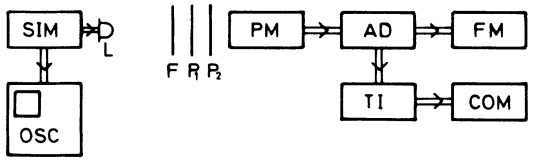

FIG. 1. Experimental setup: SIM, simulator; OSC, oscilloscope; L, photoemission diode; F, filter; P_1 and P_2, linear polarizers; PM, photomultiplier; AD, amplifier discriminator; FM, frequency meter; TI, time-interval meter; COM, computer.

TABLE I. Cases for which N samples of θ were used to evaluate $H(l,\Delta)$ with $V=0.9$. The intensity I_P is measured in photopulses/s.

Case	I_P (pulses/s)	ν_0 (Hz)	δ	τ/P	N	N_C	Δ (μs)
(A1)	10 000	10 010	$-\pi$	9	10^5	100	4
(A2)	10 000	10 010	0	8.5	10^5	100	4
(A3)	10 000	10 010	$-\pi$	9.25	10^5	100	4
(A4)	12 500	50 000	$-\pi$	49	3×10^5	500	0.5

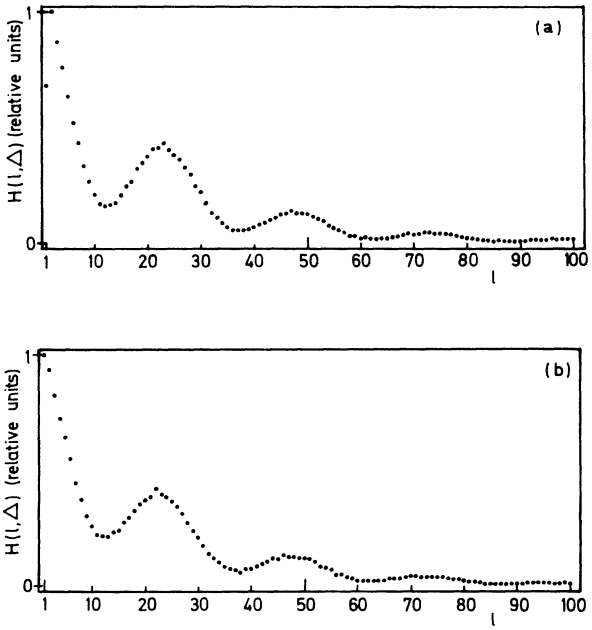

FIG. 2. Histograms [Eq. (13)] for the case (A1) in Table I: (a) experimental curve; (b) simulated curve.

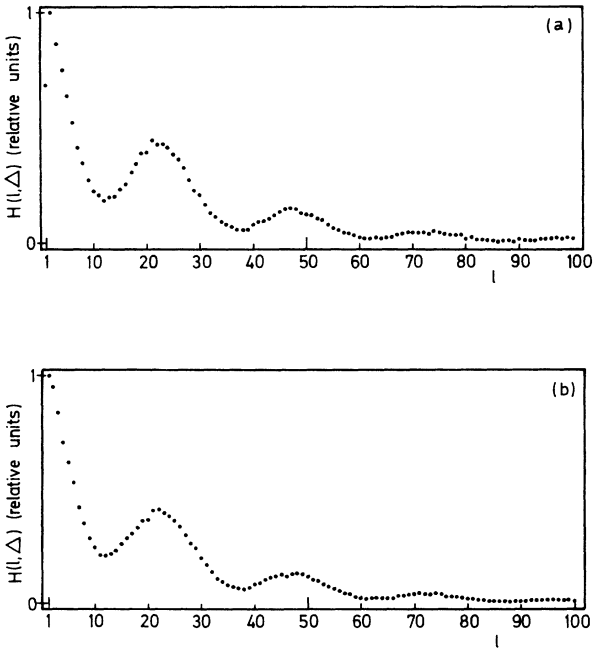

FIG. 3. Histograms for the case (A2) in Table I: (a) experimental curve; (b) simulated curve.

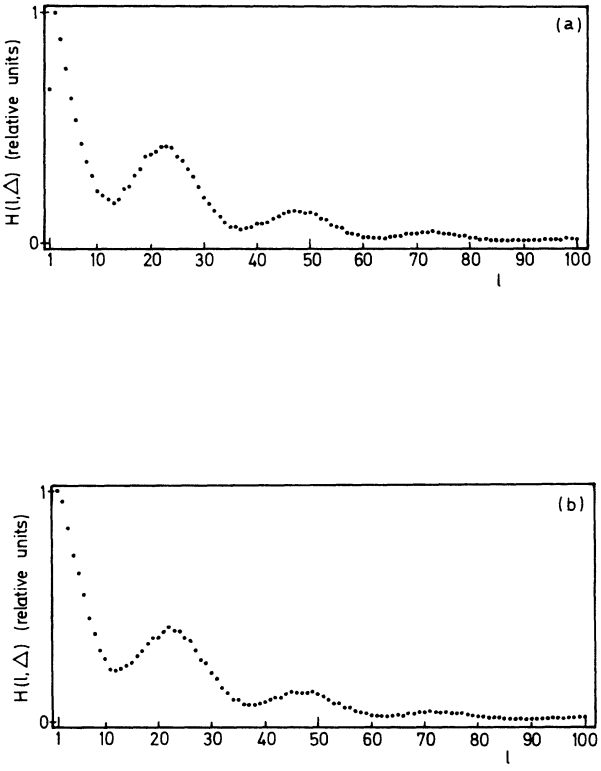

FIG. 4. Histograms for the case (A3) in Table I: (a) experimental curve; (b) simulated curve.

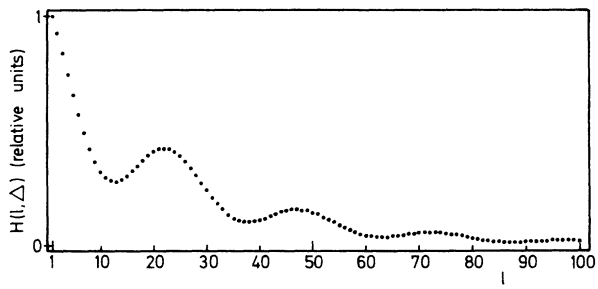

FIG. 5. Theoretical curve that corresponds to the results shown in Figs. 2–4.

method to obtain values of θ from which $H(l,\Delta)$ and $Q_F(\nu_l)$ can be obtained.

Table I shows the cases used to obtain $H(l,\Delta)$. The theoretical model used in this paper is based on the assumption that for a LDV experiment with uniform intensity beams $W(\theta)$ is not phase sensitive and therefore the time-interval probability that corresponds to an indefinite sinusoidal function can be used for $\theta \leq \tau$. Cases (A1)–(A3) are devoted to show this. In cases (A1) and (A2) the phases at $t=t_j$ [Eq. (1)] are different and the phases at $t=t_j+\tau$ are equal. In cases (A1) and (A3) the phases at $t=t_j$ are equal and the phases at $t=t_j+\tau$ are different. In these cases we have chosen small values for τ to allow us to determine the effect of phase on $W(\theta)$ with good accuracy. We used the smallest value of ν_0 (that corresponds to $P=99.9$ μs) because the phase of the signal generated by the simulator we designed can be controlled better for small values of ν_0. The results for $H(l,\Delta)$ corresponding to cases (A1)–(A3) are shown in Figs. 2–5. It can be observed that $H(l,\Delta)$ and therefore

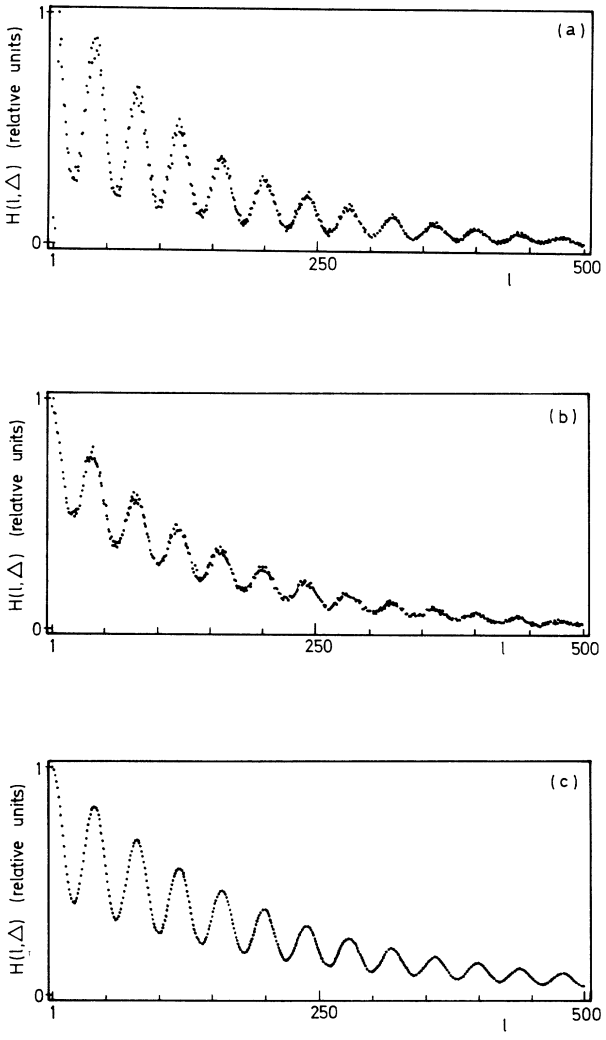

FIG. 6. Histograms for the case (A4) in Table I: (a) experimental curve; (b) simulated curve; (c) theoretical curve.

TABLE II. Cases for which N samples of θ were used to evaluate $Q_F(\nu_l)$ with $V\simeq 0.9$, $\nu_0=50\,000$ Hz, $\delta=-\pi$, and $N=10^5$. The intensity I_P is measured in photopulses/s.

Case	I_P (pulses/s)	τ/P	N_C	$\Delta\nu$ (Hz)
(B1)	50 800	9	101	1000
(B2)	48 500	29	101	1000
(B3)	5200	9	101	200
(B4)	5200	29	101	200
(B5)	5300	99	101	200
(B6)	5300	99	500	200

$W(\theta)$ are not phase sensitive and that there is accordance between experimental, simulated, and theoretical results. Case (A4) corresponds to a lower value for $I_P P$ and a larger value for τ/P than the ones corresponding to cases (A1)–(A3). A larger value of ν_0 was used in this and the following cases to diminish the effect of dark photocounts. Figure 6 shows the accordance between experimental, simulated, and theoretical curves.

Table II shows the cases used to obtain $Q_F(\nu)$. In these cases I_P and τ are varied to check the theoretical model for different experimental conditions. Once the experi-

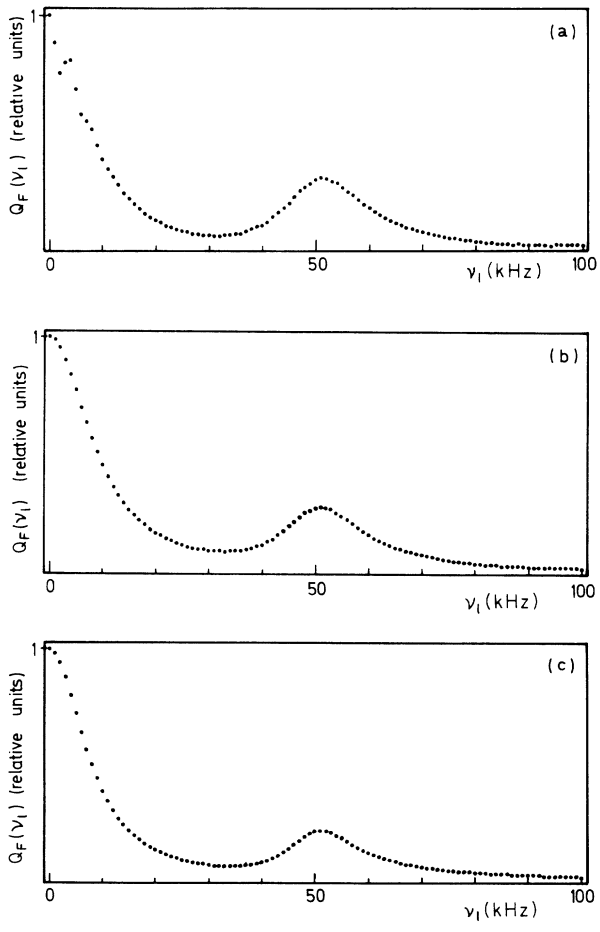

FIG. 7. Results for $Q_F(\nu_l)$ that correspond to the case (B1) in Table II: (a) experimental curve; (b) simulated curve; (c) theoretical curve.

mental and simulated curves for these cases were obtained we found that for small values of $I_P\tau$ they were wider than the theoretical ones. This is because the value of I_P is measured for an indefinite sinusoidal function, but when measuring $Q_F(\nu)$ for LDV signals the values of θ larger than τ are rejected and the mean intensity $I_\theta=\langle\theta\rangle^{-1}$ is larger than I_P. When we replaced the values of I_P in the theoretical model for the corresponding values of I_θ a good agreement between experimental, simulated, and theoretical results was obtained. Figures 7–12 show these results. It can be observed that the theoretical model for Q_F works well when the correction for the theoretical intensity is taken into account. Therefore the value of I_P in the theoretical model must be changed into I_θ. In Figs. 9–11 we can see that $Q_F(\nu)$ approaches a Lorentzian curve as $I_P\tau$ increases. In Figs. 7, 8, and 11 we can see the peaks around $\nu=0$ and $\nu=\nu_0$. The peak around $\nu=2\nu_0$ is not observed because its height is of the order of Z_M^4, whereas the height of the peak around $\nu=\nu_0$ is of the order of Z_M^2 [Eqs. (8) and (A8)] and $Z_M \ll 1$ for low intensities.

STUDY OF THE PROPERTIES OF $Q_F(\nu)$

Once the validity of the theoretical model was proved in the preceding section, we wanted to study in this one the experimental conditions for which the theoretical expression of $Q_F(\nu)$ becomes easy. As we observed in the section devoted to theory, for low intensities and a large number of interference fringes $Q_F(\nu)$ becomes a linear expansion of Lorentzian functions centered at $\nu=\pm n\nu_0$. It is interesting to determine exactly the experimental conditions that allow us to use this expansion and to know how many values of n must be taken into account. To achieve this we studied $Q_F(\nu)$ for the cases shown in Table III, where 2 is the minimum value for the mean number of photons recorded when a seeded particle passes through the fringe system.

When the heights h_0, h_1, and h_2 of the peaks around $\nu=0$, $\nu=\nu_0$, and $\nu=2\nu_0$ were calculated we found that the changes in h_1/h_0 and h_2/h_1, when τ/P is varied and $I_\theta P$ remains constant, are negligible. These relative

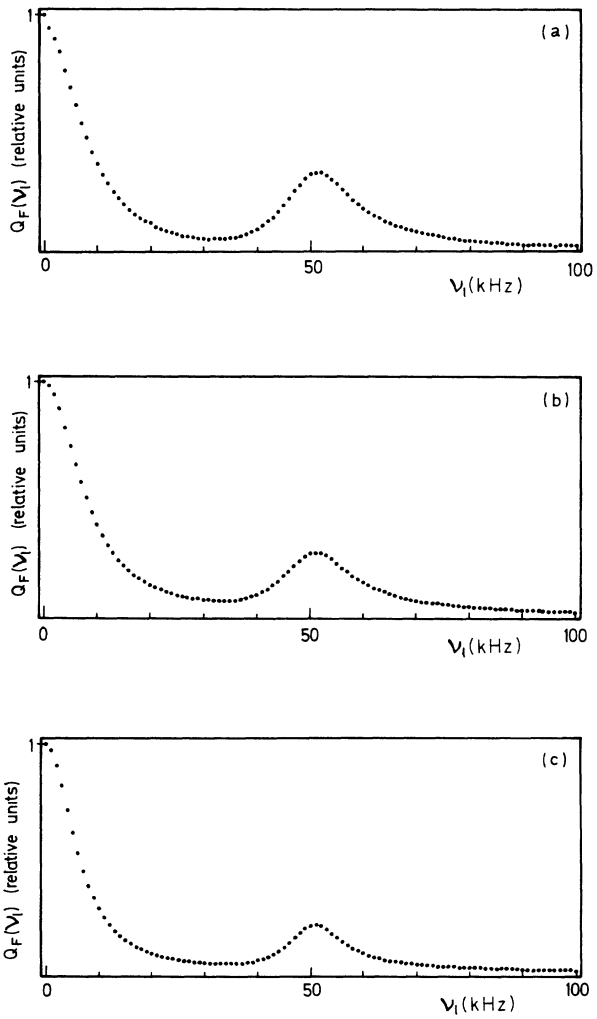

FIG. 8. Results for $Q_F(\nu_l)$ that correspond to the case (B2) in Table II: (a) experimental curve; (b) simulated curve; (c) theoretical curve.

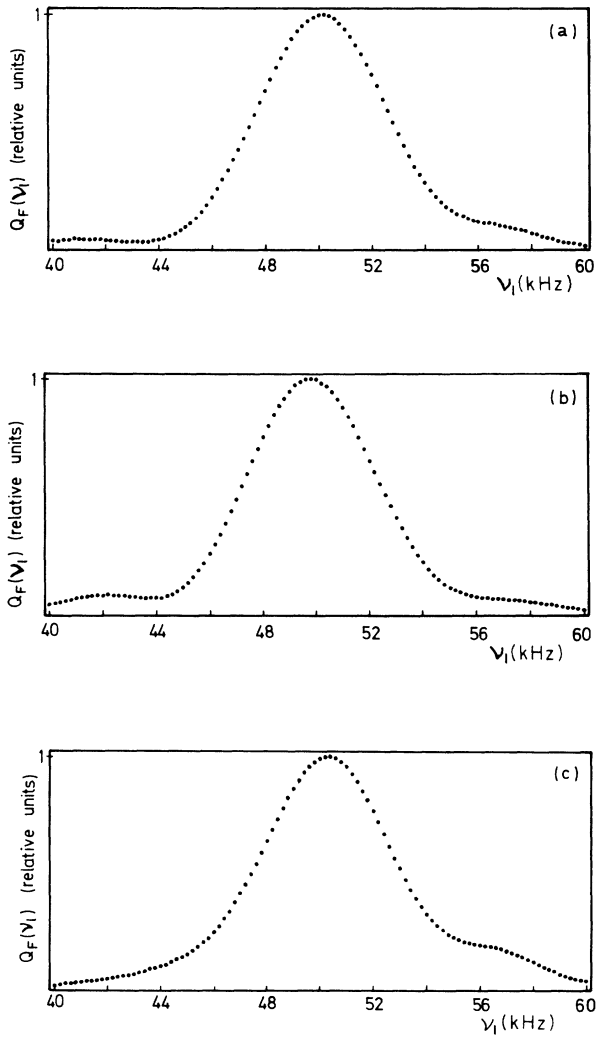

FIG. 9. Results for $Q_F(\nu_l)$ that correspond to the case (B3) in Table II: (a) experimental curve; (b) simulated curve; (c) theoretical curve.

heights are shown in Fig. 13 for the different values of $I_\theta P$. We can see that h_1/h_0 always takes a constant value, whereas h_2/h_1 decreases as $I_\theta P$ decreases, in accordance with the theoretical model. We can also see that for low intensities the peak around $\nu=2\nu_0$, and therefore the peaks around $\nu=n\nu_0$ for $n>2$, can be neglected. So the peak of Q_F around $\nu=\nu_0$ must be used to obtain ν_0 and hence the velocity of the fluid. Table IV shows the errors involved in the determination of ν_0 when it is supposed to coincide with the maximum of the peak ($e_{1\nu}$) or with the maximum of a Lorentzian curve fitted to Q_F ($e_{2\nu}$). It can be observed that $e_{1\nu}, e_{2\nu} \leq 0.1\%$ for $I_\theta P \leq 0.1$. So $I_\theta P \leq 0.1$ must be used to avoid systematic errors larger than 0.1% in the measurement of ν_0. If a larger error may be allowed this technique can be used for larger values of I_θ.

To find the experimental conditions that allow us to consider $Q_F(\nu)$ as a Lorentzian curve for ν near ν_0 we calculated the width of the peak of Q_F for these values of ν (w_1) and the width of the Lorentzian curve fitted to it (w_2). The results are shown in Table V. It can be observed that there are a variety of experimental conditions for which the difference between w_1 and w_2 is small and where Q_F can be considered as a Lorentzian curve. When $|(w_1-w_2)/w_1| \leq 0.01$ this approximation can be used with a good accuracy. The corresponding experimental conditions are approximately $I_\theta P \leq 0.2$ and $I_\theta \tau \geq 4$.

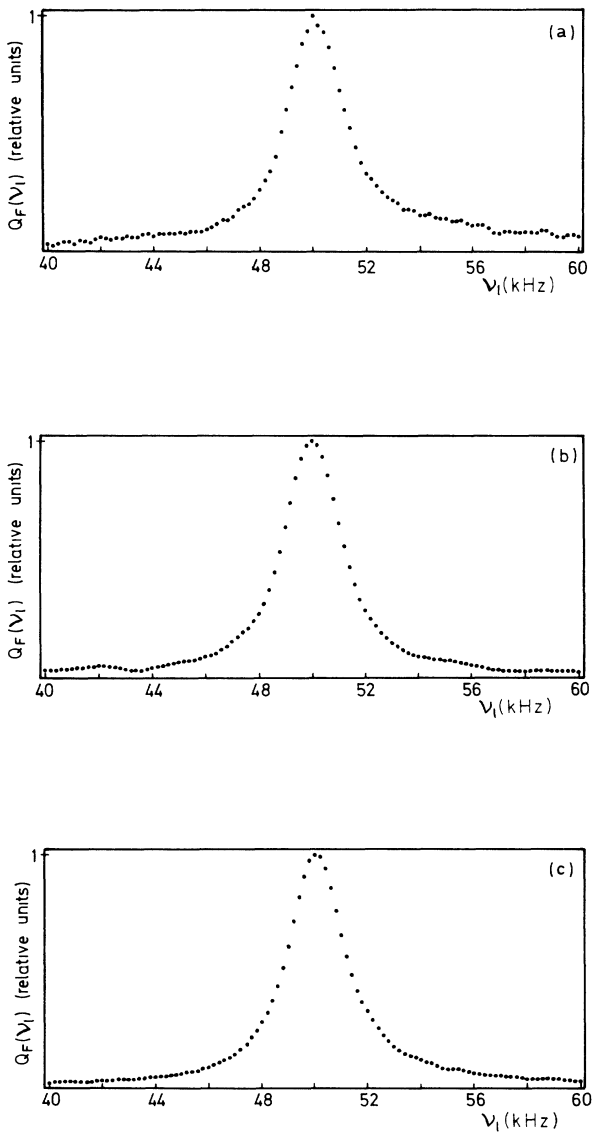

FIG. 10. Results for $Q_F(\nu_l)$ that correspond to the case (B4) in Table II: (a) experimental curve; (b) simulated curve; (c) theoretical curve.

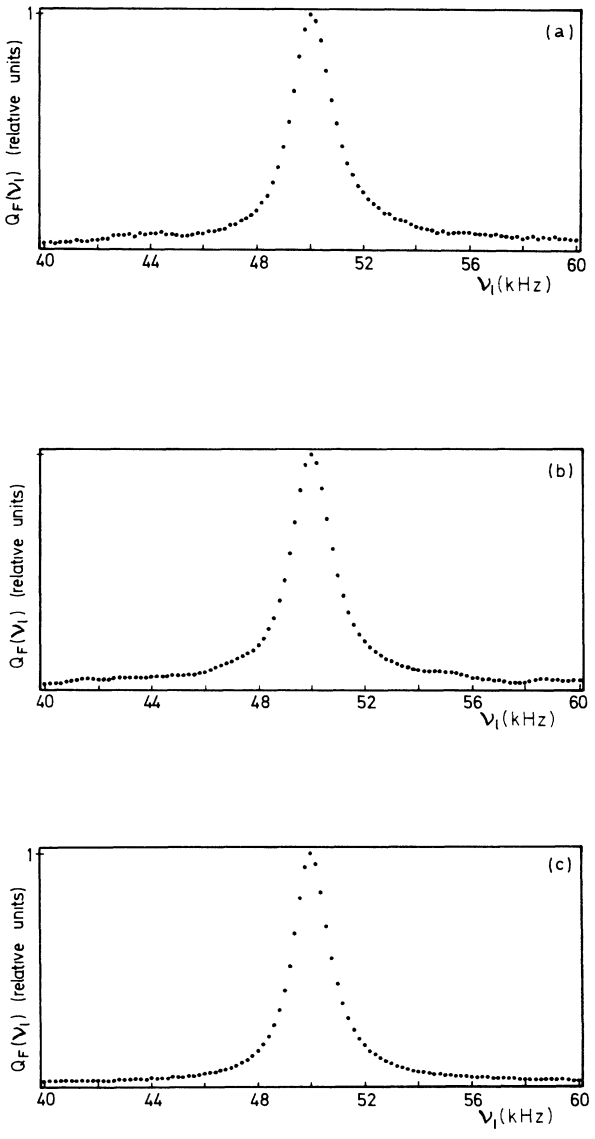

FIG. 11. Results for $Q_F(\nu_l)$ that correspond to the case (B5) in Table II: (a) experimental curve; (b) simulated curve; (c) theoretical curve.

STUDY OF THE ERRORS

Another interesting subject is to know the accuracy with which the frequency in a LDV experiment is obtained from $Q_F(\nu)$. The relative error involved in the determination of the frequency ν_0 of the signal can be calculated as

$$e_{\nu_0}=[\mathrm{var}(\nu_0)]^{1/2}/\nu_0 , \tag{14}$$

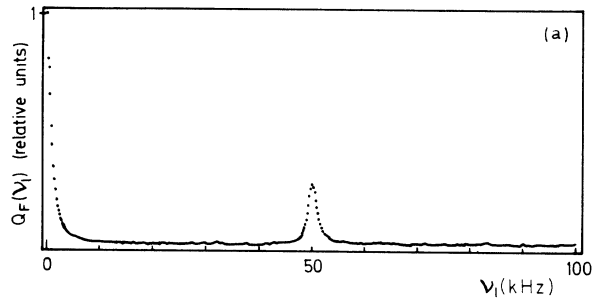

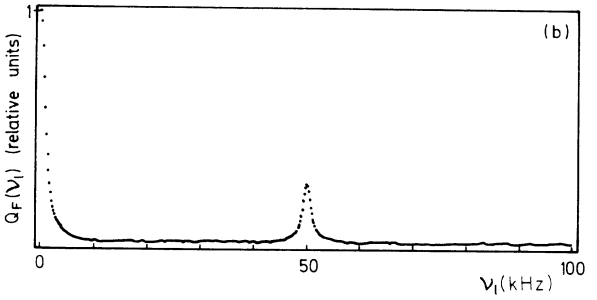

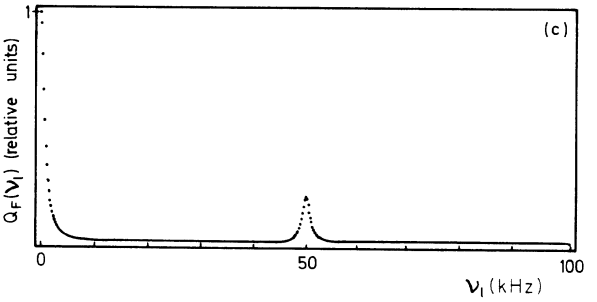

FIG. 12. Results for $Q_F(\nu_l)$ that correspond to the case (B6) in Table II: (a) experimental curve; (b) simulated curve; (c) theoretical curve.

TABLE III. Cases for which the properties of $Q_F(\nu)$ were studied from theory, for $\tau/P=10^n$ $(n=n_i,n_{i+1},\ldots,10)$.

$I_\theta P$	n_i
0.50	1
0.40	1
0.30	1
0.20	1
0.10	2
0.09	3
0.08	3
0.07	3
0.06	4
0.05	4
0.04	5
0.03	7
0.02	10

where $\mathrm{var}(\nu_0)$ is the variance of ν_0. If the experimental values of $Q_F(\nu)$ are called $Q_F^{(i)}$ when ν takes on the values ν_i $(i=1,2,\ldots,L)$, we can obtain ν_0 by minimizing the expression

$$\Delta=\sum_{i=1}^{L}[Q_F^{(i)}-Q_F(\nu_i)]^2 . \tag{15}$$

To obtain the value of ν_0 that minimizes Δ we must make

$$\sum_{i=1}^{L}[Q_F^{(i)}-Q_F(\nu_i)]\frac{\partial Q_F(\nu_i)}{\partial \nu_0}=0 . \tag{16}$$

From Eq. (16) we can deduce ν_0 as a function of $Q_F(\nu_i)$ $(i=1,2,\ldots,L)$. Hence if the law of error propagation is applied, $\mathrm{var}(\nu_0)$ can be easily obtained as

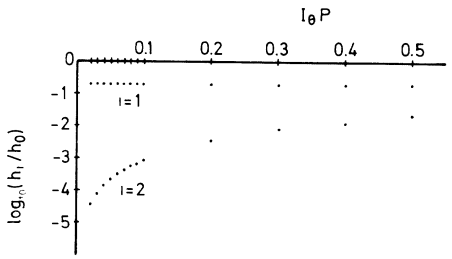

FIG. 13. Values of $\log(h_1/h_0)$ and $\log(h_2/h_0)$; h_0, h_1, and h_2 being the heights of the peaks of Q_F around $\nu=0$, $\nu=\nu_0$, and $\nu=2\nu_0$.

$$\mathrm{var}(\nu_0)=\left[\sum_{i=1}^{L}\left[\frac{\partial Q_F(\nu_i)}{\partial\nu_0}\right]^2\right]^{-2}\left[\sum_{i=1}^{L}\left[\frac{\partial Q_F(\nu_i)}{\partial\nu_0}\right]^2\mathrm{var}[Q_F(\nu_i)]+\sum_{\substack{i,j=1\\ i\neq j}}^{L}\left[\frac{\partial Q_F(\nu_i)}{\partial\nu_0}\right]\left[\frac{\partial Q_F(\nu_j)}{\partial\nu_0}\right]\mathrm{cov}[Q_F(\nu_i),Q_F(\nu_j)]\right], \tag{17}$$

where $\mathrm{cov}[Q_F(\nu_i),Q_F(\nu_j)]$ is the covariance of $Q_F(\nu_i)$ and $Q_F(\nu_j)$.

If we recall that an estimation $\hat{Q}_F(\nu)$ of $Q_F(\nu)$ is obtained by making N samples of θ and performing the operation

$$\hat{Q}_F(\nu)=\frac{1}{N}\sum_{K=1}^{N}\cos(2\pi\nu\theta_K), \tag{18}$$

then the covariances can be evaluated using the definition, that is,

$$\mathrm{cov}[Q_F(\nu_i),Q_F(\nu_j)]=\langle[\hat{Q}_F(\nu_i)-\langle\hat{Q}_F(\nu_i)\rangle][\hat{Q}_F(\nu_j)-\langle\hat{Q}_F(\nu_j)\rangle]\rangle=\langle\hat{Q}_F(\nu_i)\hat{Q}_F(\nu_j)\rangle-Q_F(\nu_i)Q_F(\nu_j). \tag{19}$$

We obtain immediately

$$\langle\hat{Q}_F(\nu_i)\hat{Q}_F(\nu_j)\rangle=\frac{1}{N^2}\left[\sum_{K=1}^{N}\langle\cos(2\pi\nu_i\theta_K)\cos(2\pi\nu_j\theta_K)\rangle+\sum_{\substack{K,l=1\\ K\neq l}}^{N}\langle\cos(2\pi\nu_i\theta_K)\cos(2\pi\nu_j\theta_l)\rangle\right]$$

$$=\frac{1}{N^2}\left[\frac{N}{2}[Q_F(\nu_i-\nu_j)+Q_F(\nu_i+\nu_j)]+N(N-1)Q_F(\nu_i)Q_F(\nu_j)\right]. \tag{20}$$

TABLE IV. Errors involved in the determination of ν_0 when obtained from the maximum of $Q_F(\nu)$ around ν_0 ($e_{1\nu}$) or from the maximum of a Lorentzian curve fitted to $Q_F(\nu)$ ($e_{2\nu}$).

	τ/P										
$I_\theta P$	10	20	30	40	50	60	70	80	90	100	Error (%)
0.50	0.73	0.62	0.61	0.61	0.61	0.61	0.61	0.61	0.61	0.61	$e_{1\nu}$
	1.17	1.17	1.17	1.17	1.17	1.17	1.17	1.17	1.17	1.17	$e_{2\nu}$
0.40	0.57	0.40	0.40	0.40	0.40	0.40	0.40	0.40	0.40	0.40	$e_{1\nu}$
	0.79	0.77	0.77	0.77	0.77	0.77	0.77	0.77	0.77	0.77	$e_{2\nu}$
0.30	0.47	0.25	0.23	0.23	0.23	0.23	0.23	0.23	0.23	0.23	$e_{1\nu}$
	0.50	0.44	0.44	0.44	0.44	0.44	0.44	0.44	0.44	0.44	$e_{2\nu}$
0.20	0.41	0.15	0.11	0.10	0.10	0.10	0.10	0.10	0.10	0.10	$e_{1\nu}$
	0.34	0.21	0.20	0.20	0.20	0.20	0.20	0.20	0.20	0.20	$e_{2\nu}$
0.10		0.10	0.05	0.04	0.03	0.03	0.03	0.03	0.03	0.03	$e_{1\nu}$
		0.09	0.06	0.05	0.05	0.05	0.05	0.05	0.05	0.05	$e_{2\nu}$
0.09			0.05	0.03	0.03	0.02	0.02	0.02	0.02	0.02	$e_{1\nu}$
			0.05	0.04	0.04	0.04	0.04	0.04	0.04	0.04	$e_{2\nu}$
0.08			0.05	0.03	0.02	0.02	0.02	0.02	0.02	0.02	$e_{1\nu}$
			0.04	0.04	0.03	0.03	0.03	0.03	0.03	0.03	$e_{2\nu}$
0.07			0.05	0.03	0.02	0.02	0.02	0.01	0.01	0.01	$e_{1\nu}$
			0.04	0.03	0.03	0.03	0.02	0.02	0.02	0.02	$e_{2\nu}$
0.06				0.03	0.02	0.01	0.01	0.01	0.01	0.01	$e_{1\nu}$
				0.02	0.02	0.02	0.02	0.02	0.02	0.02	$e_{2\nu}$
0.05				0.03	0.02	0.01	0.01	0.01	0.01	0.01	$e_{1\nu}$
				0.02	0.02	0.01	0.01	0.01	0.01	0.01	$e_{2\nu}$
0.04					0.02	0.01	0.01	0.01	0.01	0.01	$e_{1\nu}$
					0.01	0.01	0.01	0.01	0.01	0.01	$e_{2\nu}$
0.03							0.01	0.01	0.01	0.00	$e_{1\nu}$
							0.01	0.01	0.01	0.01	$e_{2\nu}$
0.02										0.00	$e_{1\nu}$
										0.00	$e_{2\nu}$

From Eqs. (19) and (20) $\mathrm{cov}[Q_F(\nu_i), Q_F(\nu_j)]$ and therefore $\mathrm{var}Q_F(\nu_i)$ can be evaluated.

By using Eqs. (17), (19), (20), and the theoretical expressions for $Q_F(\nu)$, we calculated e_{ν_0} for the cases in Table III, when $Q_F(\nu)$ is obtained from 1000 time intervals ($N=1000$) for 100 values of ν ($L=100$). The results are shown in Table VI. It can be observed that the changes in e_{ν_0} as τ/P is varied are generally negligible. Furthermore, the values of e_{ν_0} are small and decrease as $I_\theta P$ does. The values of e_{ν_0} can also be calculated as a function of I_P (the mean intensity in an oscillation of the LDV signal). To do this we must obtain the value I_θ of the corrected intensity. To obtain these values of I_θ ($I_\theta=\langle\theta\rangle^{-1}$) we made computer simulations of the corresponding LDV signals. The results are shown in Table VII. It can be observed that e_{ν_0} decreases as τ/P and $I_P P$ do and that these values of e_{ν_0} are small.

CONCLUSIONS

In this paper we have obtained a theoretical model for the Fourier transform $Q_F(\nu)$ of the time-interval probability corresponding to the signal from a differential LDV system where two laser beams with a uniform intensity are used to study a fluid with a constant velocity. The validity of this model was verified experimentally and by means of a computer-simulation method. From the theoretical model it was found that for low intensities there is a wide variety of experimental situations for which $Q_F(\nu)$ can be expressed with good accuracy as a linear expansion of two Lorentzian curves. One of these Lorentzians is centered at the frequency ν_0 of the LDV signal and can be used to measure ν_0 and therefore the velocity of the fluid. The expected values of the error in the determination of ν_0 when a low number of time intervals are measured ($N=1000$) are small and decrease as the intensity of the light beam does. Since the error involved in the information obtained from the intensity autocorrelation function (used in LDV for low intensities) increases[5] as the intensity decreases, we can conclude that the measurement of $Q_F(\nu)$ is a useful technique in LDV for very low intensities.

ACKNOWLEDGMENTS

This work was supported by the Consejo Asesor de Investigación de la Diputación General de Aragón (Pro-

TABLE V. Relative widths of the peak of Q_F around $\nu=\nu_0$ (w_1) and of the Lorentzian curve fitted to this peak (w_2).

	τ/P										
$I_\theta P$	10	20	30	40	50	60	70	80	90	100	Relative widths
0.50	0.1641	0.1642	0.1642	0.1642	0.1642	0.1642	0.1642	0.1642	0.1642	0.1642	w_1
	0.1728	0.1727	0.1727	0.1727	0.1727	0.1727	0.1727	0.1727	0.1727	0.1727	w_2
0.40	0.1310	0.1301	0.1300	0.1300	0.1300	0.1300	0.1300	0.1300	0.1300	0.1300	w_1
	0.1351	0.1341	0.1347	0.1347	0.1347	0.1347	0.1347	0.1347	0.1347	0.1347	w_2
0.30	0.1045	0.0967	0.0966	0.0966	0.0966	0.0966	0.0966	0.0966	0.0966	0.0966	w_1
	0.1010	0.0986	0.0986	0.0986	0.0986	0.0986	0.0986	0.0986	0.0986	0.0986	w_2
0.20	0.0845	0.0648	0.0640	0.0640	0.0640	0.0640	0.0640	0.0640	0.0640	0.0640	w_1
	0.0730	0.0649	0.0646	0.0646	0.0646	0.0646	0.0646	0.0646	0.0646	0.0646	w_2
0.10		0.0425	0.0347	0.0323	0.0318	0.0318	0.0319	0.0319	0.0318	0.0318	w_1
		0.0363	0.0328	0.0321	0.0320	0.0320	0.0320	0.0320	0.0320	0.0320	w_2
0.09			0.0326	0.0297	0.0287	0.0286	0.0287	0.0287	0.0287	0.0287	w_1
			0.0300	0.0290	0.0288	0.0287	0.0287	0.0287	0.0287	0.0287	w_2
0.08			0.0307	0.0272	0.0258	0.0254	0.0254	0.0255	0.0255	0.0255	w_1
			0.0274	0.0260	0.0257	0.0256	0.0255	0.0255	0.0255	0.0255	w_2
0.07			0.0289	0.0250	0.0232	0.0225	0.0223	0.0223	0.0223	0.0223	w_1
			0.0249	0.0232	0.0226	0.0224	0.0223	0.0223	0.0223	0.0223	w_2
0.06				0.0230	0.0209	0.0197	0.0193	0.0191	0.0191	0.0191	w_1
				0.0205	0.0197	0.0193	0.0192	0.0191	0.0191	0.0191	w_2
0.05				0.0212	0.0188	0.0174	0.0166	0.0162	0.0160	0.0159	w_1
				0.0181	0.0169	0.0164	0.0161	0.0160	0.0160	0.0159	w_2
0.04					0.0170	0.0154	0.0143	0.0136	0.0132	0.0129	w_1
					0.0145	0.0137	0.0132	0.0130	0.0129	0.0128	w_2
0.03							0.0124	0.0115	0.0109	0.0105	w_1
							0.0107	0.0103	0.0100	0.0098	w_2
0.02										0.0085	w_1
										0.0072	w_2

TABLE VI. Values of e_{v_0}, for $L=100$ and $N=1000$, when τ/P and $I_\theta P$ are varied.

	τ/P									
$I_\theta P$	10	20	30	40	50	60	70	80	90	100
0.50	1.12	1.13	1.13	1.13	1.13	1.13	1.13	1.13	1.13	1.13
0.40	0.88	0.88	0.88	0.88	0.88	0.88	0.88	0.88	0.88	0.88
0.30	0.66	0.65	0.65	0.65	0.65	0.65	0.65	0.65	0.65	0.65
0.20	0.49	0.42	0.42	0.43	0.43	0.43	0.43	0.43	0.43	0.43
0.10		0.24	0.21	0.21	0.21	0.21	0.21	0.21	0.21	0.21
0.09			0.20	0.19	0.19	0.19	0.19	0.19	0.19	0.19
0.08			0.18	0.17	0.17	0.17	0.17	0.17	0.17	0.17
0.07			0.17	0.15	0.15	0.15	0.15	0.15	0.15	0.15
0.06				0.14	0.13	0.13	0.13	0.13	0.13	0.13
0.05				0.12	0.11	0.11	0.11	0.10	0.11	0.10
0.04					0.10	0.09	0.09	0.09	0.08	0.08
0.03							0.07	0.07	0.07	0.06
0.02										0.05

ject No. CB 2/85). The authors wish also to express their sincere thanks to Dr. J. Tornos for help in experimental measurements and to Mr. M. Sevilla for help in electronic simulator building.

APPENDIX

For small values of I_P [Eq. (1)] the values of Z [Eq. (5)] are small and we can use the expansions[7]

$$I_0(Z)=\sum_{K=0}^{\infty}(Z/2)^{2K}/(K!)^2\ , \tag{A1}$$

$$I_1(Z)=\sum_{K=0}^{\infty}(Z/2)^{2K+1}/[K!(K+1)!]\ . \tag{A2}$$

To evaluate the powers of Z we can use[7] the well-known expressions

$$\sin^{2r-1}(X)=\frac{(-1)^{r-1}}{2^{2r-2}}\sum_{s=0}^{r-1}(-1)^s\binom{2r-1}{s}\sin[2(r-s)-1]\times X(r>0)\ , \tag{A3}$$

$$\sin^{2r}(X)=\frac{1}{2^{2r}}\binom{2r}{r}+\frac{(-1)^r}{2^{2r-1}}\sum_{s=0}^{r-1}(-1)^s\binom{2r}{s}\cos[2(r-s)]\times X(r>0)\ . \tag{A4}$$

From the preceding relations the following expression is easily obtained:

$$I_0(\theta)=1+\sum_{K=1}^{\infty}\frac{(Z_M/2)^{2K}}{(K!)^2}\left[\frac{1}{2^{2K}}\binom{2K}{K}+\frac{(-1)^K}{2^{2K-1}}\sum_{s=0}^{K-1}(-1)^s\binom{2K}{s}\cos[(K-s)\omega_0\theta]\right]\ , \tag{A5}$$

TABLE VII. Values of e_{v_0}, for $L=100$ and $N=1000$, when τ/P and $I_P P$ are varied.

	τ/P									
$I_\theta P$	10	20	30	40	50	60	70	80	90	100
0.50	1.42	1.26	1.21	1.19	1.18	1.17	1.16	1.15	1.15	1.15
0.40	1.20	1.02	0.97	0.94	0.93	0.92	0.92	0.91	0.91	0.91
0.30	1.00	0.77	0.73	0.71	0.70	0.69	0.68	0.68	0.67	0.67
0.20	0.89	0.56	0.50	0.49	0.47	0.46	0.46	0.45	0.45	0.45
0.10		0.43	0.31	0.28	0.26	0.25	0.25	0.24	0.24	0.23
0.09			0.30	0.26	0.24	0.23	0.22	0.22	0.22	0.21
0.08			0.29	0.24	0.22	0.21	0.20	0.20	0.20	0.19
0.07			0.28	0.23	0.20	0.19	0.18	0.18	0.17	0.17
0.06				0.21	0.19	0.17	0.16	0.16	0.15	0.15
0.05				0.21	0.17	0.15	0.14	0.14	0.13	0.13
0.04					0.17	0.14	0.13	0.12	0.11	0.11
0.03							0.12	0.11	0.10	0.09
0.02										0.08

$$I_1(\theta)=(Z_M/2)\sin(\omega_0\theta/2)$$
$$\times\left\{1+\sum_{K=1}^{\infty}\frac{(Z_M/2)^{2K}}{K!(K+1)!}\left[\frac{1}{2^{2K}}\begin{bmatrix}2K\\K\end{bmatrix}+\frac{(-1)^K}{2^{2K-1}}\sum_{s=0}^{K-1}(-1)^s\begin{bmatrix}2K\\s\end{bmatrix}\cos[(K-s)\omega_0\theta]\right]\right\}. \tag{A6}$$

If $l=K-s$ is used in Eqs. (A5) and (A6), $Y(\theta)$ [Eq. (4)] can be expressed as

$$\begin{aligned}Y(\theta)=&1+(1+V^2/2)\sum_{K=1}^{\infty}A_K-(V^2/2)\sum_{K=1}^{\infty}B_K+(V^2/2)\left[1+\sum_{K=1}^{\infty}A_K\right]\cos(\omega_0\theta)\\&-(Z_MV/2)\left[1+\sum_{K=1}^{\infty}B_K\right]\sin(\omega_0\theta)+(1+V^2/2)\sum_{K=1}^{\infty}C_K\sum_{l=1}^{K}(-1)^l\begin{bmatrix}2K\\K-l\end{bmatrix}\cos(l\omega_0\theta)\\&-(V^2/2)\sum_{K=1}^{\infty}D_K\sum_{l=1}^{K}(-1)^l\begin{bmatrix}2K\\K-l\end{bmatrix}\cos(l\omega_0\theta)+(V^2/2)\sum_{K=1}^{\infty}C_K\sum_{l=1}^{K}(-1)^l\begin{bmatrix}2K\\K-l\end{bmatrix}\cos(\omega_0\theta)\cos(l\omega_0\theta)\\&-(Z_MV/2)\sum_{K=1}^{\infty}D_K\sum_{l=1}^{K}(-1)^l\begin{bmatrix}2K\\K-l\end{bmatrix}\sin(\omega_0\theta)\cos(l\omega_0\theta)\,,\end{aligned} \tag{A7}$$

where

$$A_K=\frac{(Z_M/4)^{2K}(2K)!}{(K!)^4}\,,\quad B_K=\frac{(Z_M/4)^{2K}(2K)!}{(K!)^3(K+1)!}\,,\quad C_K=\frac{2(Z_M/4)^{2K}}{(K!)^2}\,,\quad D_K=\frac{2(Z_M/4)^{2K}}{K!(K+1)!}\,. \tag{A8}$$

[1]*Photon Correlation Techniques in Fluid Mechanics*, edited by E. O. Schulz-Dubois (Springer, New York, 1983).
[2]M. A. Rebolledo, R. J. López, and F. Moreno, Opt. Commun. **52**, 81 (1984).
[3]F. Moreno, M. A. Rebolledo, and R. J. López, Phys. Rev. A **33**, 416 (1986).
[4]M. Quintanilla and A. M. Frutos, Appl. Opt. **20**, 879 (1981).
[5]B. Saleh, *Photoelectron Statistics* (Springer, Berlin, 1978).
[6]F. C. Van Rijswijk and C. Smit, Physica (Utrecht) **49**, 549 (1970).
[7]I. S. Gradshteyn and I. M. Rizhik, *Tables of Integrals, Series and Products* (Academic, Orlando, 1980).